The electronic structure of Hf_2Co: perturbed angular correlation study and first principle calculations

2004 J. Phys.: Condens. Matter 16 3015

(http://iopscience.iop.org/0953-8984/16/18/002)

INSTITUTE OF PHYSICS PUBLISHING JOURNAL OF PHYSICS: CONDENSED MATTER

J. Phys.: Condens. Matter **16** (2004) 3015–3026 PII: S0953-8984(04)71452-6

The electronic structure of Hf_2Co: perturbed angular correlation study and first principle calculations

B Cekić, N Ivanović, V Koteski, S Koički and M Manasijević

Institute of Nuclear Sciences—Vinča, POB 522, 11001 Belgrade, Serbia and Montenegro

Received 5 November 2003, in final form 1 March 2004
Published 23 April 2004
Online at stacks.iop.org/JPhysCM/16/3015
DOI: 10.1088/0953-8984/16/18/002

Abstract

The results of high resolution TDPAC measurements of electric quadrupole interaction (EQI) at the ^{181}Ta probe ion in the polycrystalline intermetallic compound Hf_2Co of the Ti_2Ni structure type, in a temperature range from 77 to 1200 K, are presented. The results show the presence of two independent EQIs. At room temperature their frequencies are $\omega_{Q_1} = 36(3)$ Mrad s^{-1} at the 16c, and $\omega_{Q_2} = 230(3)$ Mrad s^{-1} at the 48f position. The low frequency interaction is characterized by an unusual temperature dependence which shows a pronounced maximum. The temperature dependence of all relevant physical parameters (the electric field gradient (EFG) principal component V_{ZZ}, the EFG distribution parameter δ, the asymmetry parameter η, and the fractions of ions contributing to the specific interaction) are also presented. In addition, the EFG parameters of the same structure are calculated using the full-potential linearized augmented plane-wave (FP-LAPW) method as implemented in the WIEN97 package, and the results are compared with the measured data and some previous calculations obtained using the full-potential linear muffin-tin orbital (FP-LMTO) method in the atomic sphere approximation (ASA).

1. Introduction

The intermetallic compound Hf_2Co belongs to the group of binary systems formed between an early (Ti, Zr, Hf) and a late transition metal (Fe, Co, Pd, Pt). Among other reasons, they have been investigated as systems interesting for hydrogen storage [1], since they are able to form hydrides in hydrogen-to-metal atom ratios H/M $\geqslant 1$ at rather low temperatures ($T \sim 300\,^{\circ}$C) and pressures [2, 3].

Several techniques have been used to investigate Hf-Co phases and their hydrides, including muon spin relaxation (μSR) [2], and the time-differential perturbed-angular-correlation (TDPAC) technique [4]. By measuring the EQI between the nuclear quadrupole moment Q of the radioactive probe and the EFG tensor at the ion probe site, the TDPAC technique provides a way to determine the charge distribution around the probe atom in a

given sample. Usually, the EFG tensor is characterized by its largest component V_{ZZ} and the asymmetry parameter $\eta = |V_{XX} - V_{YY}|/V_{ZZ}$.

The TDPAC results obtained in this work are quite uncommon for a metallic system, and require further elaboration. Similar peculiarities are found for the isostructural compounds Hf_2Fe [14] and Hf_2Rh [16]. For that reason, apart from the measured and calculated hyperfine parameters, we also present the electronic structure, density of states and valence charge density of Hf_2Co, and discuss its bonding and structural aspects. We also address the role of the tantalum probe, as an impurity atom, on the EFG. To our best knowledge, these are the first complete *ab initio* calculations of the electronic structure of this compound.

This paper is organized as follows. In section 2 we discuss some of the structural aspects of Hf_2Co. In section 3 we present the results of our high-resolution TDPAC measurements in the temperature range from 78 to 1200 K at the ^{181}Ta ion probe 133–482 keV gamma cascade. Section 4 contains the results of the corresponding calculations using the FP-LAPW method performed with the WIEN97 software package [5]. We compare the experimental and theoretical results and give a summary in section 5.

2. Structural aspects of Hf_2Co

The conventional unit cell of Hf_2Co consists of 96 atoms (space group $Fd\bar{3}m$). To reduce the computational burden of our calculations we used the primitive unit cell, constructed out of 24 atoms [8 formula units (fu) of Hf_2Co]. The cell parameter a was experimentally determined as 12.084(1) Å for the unannealed, and 12.066(1) Å for the annealed sample [6]. 4 atoms of the primitive unit cell are located at the 16c (Hf1), and 12 at the 48f (Hf2) positions, while 8 Co atoms are at the 32e position. This structure possesses two internal parameters u, and v, which determine the non-equivalent position of Co [(u, u, u)], and Hf2 [$(v, 1/4, 1/4)$]—both given in units of a.

In the upper part of figure 1 two different views of the local coordination (12 nearest neighbour (NN) atoms, divided in two sub-shells with 6 Co and 6 Hf atoms) around Hf1 are given. The Hf1 lattice site possesses relatively high point-group symmetry ($\bar{3}m$), and the threefold axis of rotation is clearly visible (figure 1).

As a consequence, the corresponding EFG should have axial symmetry: for example, for the Hf1 atom located at the origin of the conventional unit cell the symmetry axis points in the $\langle 111 \rangle$ crystallographic direction. In the bottom part of figure 1 the arrangement of atoms in the vicinity of Hf2 is presented. The point group of this lattice site is $mm2$ with the twofold axis of rotation indicated. Owing to the rather low point-group symmetry, we expect a nonzero asymmetry parameter η for this lattice site.

3. Experimental details

3.1. Source preparation

Starting from high-purity cobalt (99.98%) and hafnium (99.97%, except 2% of Zr), an Hf_2Co bulk specimen of weight of about 5 g was synthesized in an RF-induction furnace under controlled argon atmosphere, and remelted several times to ensure homogenization. The polycrystalline compound Hf_2Co occurred at about 33% Co. The single-phase cubic structure of the Ti_2Ni structure type with the $Fd\bar{3}m$ space group was confirmed by x-ray powder diffraction measurements [6, 12] at room temperature (RT).

Hf_2Co samples of several milligrams, with negligible self-absorption of gamma rays, were sealed in a double quartz ampoule evacuated to 10^3 Pa, and the ^{181}Hf isotope was activated in

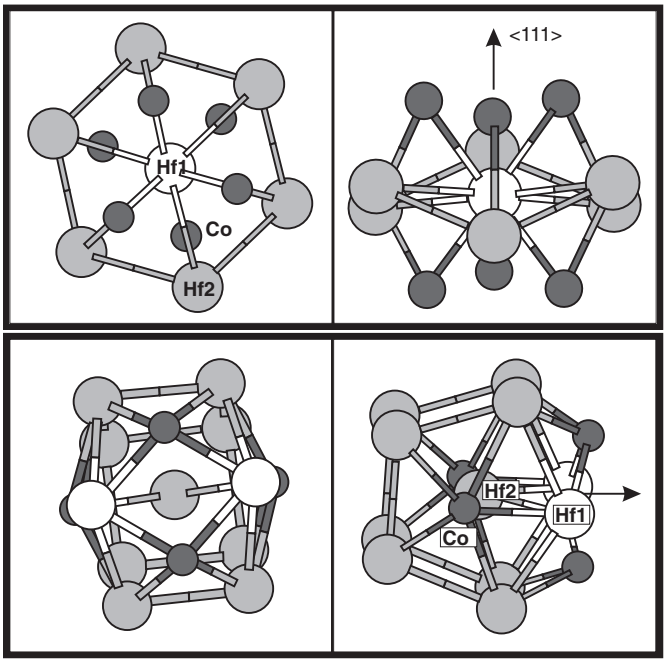

Figure 1. The local coordination around the Hf1 (top) and Hf2 (bottom) lattice sites in the Hf_2Co structure.

a reactor with high neutron flux ($\sim 10^{15}$ cm^{-2} s^{-1}). The post-irradiation annealing at 900 °C for 12 days repaired neutron irradiation damages and significantly improved the structure of the TDPAC pattern, compared with the unannealed sample.

3.2. Experimental set-up

The TDPAC measurements were performed on the 133–482 keV gamma cascade of ^{181}Ta, which is populated through the 42 days β-decay of the ^{181}Hf isotope. A high-resolution, two-detector coincidence set-up with BaF_2 crystal scintillators and XP-2020Q photomultipliers was used. The positive timing signal was derived from the seventh dynode and further processed by an Ortec VT-120 fast amplifier (rise time < 1 ns, gain > 200) before feeding a standard constant-fraction discriminator. The energy signal was taken from the ninth dynode. The time resolution of the coincidence system was preserved at a level of about 0.5 ns throughout the experiment. The coincidence measurements at high and low temperatures were performed with a low gamma-ray scattering furnace and liquid-nitrogen Dewar, respectively.

3.3. Experimental results

The experimental perturbation function $R(t)$ was derived from TDPAC spectra measured at two angles, $W(90°, t)$ and $W(180°, t)$ [9]:

$$R(t) = 2\frac{N(180°) - N(90°)}{N(180°) + 2N(90°)}. \tag{1}$$

It could be represented as $R(t) = A_{22}G_{22}(t)$. A_{22} is the angular correlation and $G_{22}(t)$ is the perturbation factor of a randomly oriented static EQI. $G_{22}(t)$ for the probe ion with the

Table 1. EQI parameters of the ^{181}Ta probe in Hf_2Co at the 16c and 48f positions. $Q = 2.36(5) \times 10^{-24}$ cm^2 is the value of the nuclear quadrupole moment used for the V_{ZZ} calculation. The interaction frequencies ω_Q are given in Mrad s^{-1}, while the values of V_{ZZ} are given in units of 10^{17} V cm^{-2}.

T (K)	ω_Q	η	δ	F_i	V_{ZZ}
16c					
78	23(3)	0.74(20)	0.29(20)	0.08(1)	2.4(3)
295	36(3)	0.57(20)	0.14(10)	0.13(1)	3.7(3)
573	32(2)	0.54(12)	0.14(7)	0.21(1)	3.3(2)
773	24(3)	0.79(20)	0.20(12)	0.23(1)	2.5(3)
1023	26(1)	0.56(10)	0.00(20)	0.20(1)	2.7(1)
1173	26(1)	0.42(2)	0.05(8)	0.20(1)	2.7(1)
48f					
78	251(3)	0.04(5)	0.16(2)	0.66(1)	26.1(3)
295	230(3)	0.00(1)	0.12(10)	0.78(1)	23.9(3)
573	179(1)	0.29(1)	0.04(5)	0.60(1)	18.6(1)
773	151(1)	0.29(1)	0.03(4)	0.59(1)	15.7(1)
1023	159(1)	0.30(1)	0.03(1)	0.62(1)	16.5(1)
1173	151(1)	0.28(1)	0.04(5)	0.53(1)	15.7(1)

intermediate level spin $I = 5/2$ has the form

$$G_{22}(t) = a_{20} + \sum_{n=1}^{3} a_{2n} \exp\left(-\frac{\omega_n^2 \tau_R^2}{2}\right) \exp(-\delta\omega_n t) \cos(\omega_n t). \tag{2}$$

The coefficients a_{20} and a_{2n} are functions of the asymmetry parameter η, the frequencies ω_n depend on ω_Q and the asymmetry parameter η. The quadrupole interaction frequency ω_Q is defined as

$$\omega_Q = \frac{eQV_{ZZ}}{4I(2I-1)\hbar}, \tag{3}$$

where Q is the spectroscopic quadrupole moment. The spin value I of the isomeric state of ^{181}Ta is 5/2. The damping of the oscillation amplitudes a_{2n} is introduced through a finite time resolution τ_R of the TDPAC apparatus, and the EFG distribution parameter δ is the Lorentzian distribution width and reflects the inhomogeneity of the charge distribution around the probe atom.

Since in this case the ^{181}Ta nuclei experiences more than one hyperfine interaction, fitting is made by the expression

$$G_{22}(t) = \sum_i F_i G_{22}^i(t), \tag{4}$$

where F_i is the fraction of decaying ^{181}Ta nuclei at the ith lattice site, experiencing ith hyperfine interaction.

The TDPAC coincidence spectra $R(t)$ at six characteristic temperatures in the temperature range from 78 to 1200 K are presented in figure 2. The interaction frequencies are connected with the two crystallographic sites (Hf1 and Hf2) in the Hf_2Co unit cell. The measured values of two remarkably different EQIs, associated with these inequivalent crystallographic sites in the Ti_2Ni type lattice, are presented in table 1 and figure 5. The ratio of the EQI intensities at the two sites varies from 11 at 78 K to 6 at 1173 K.

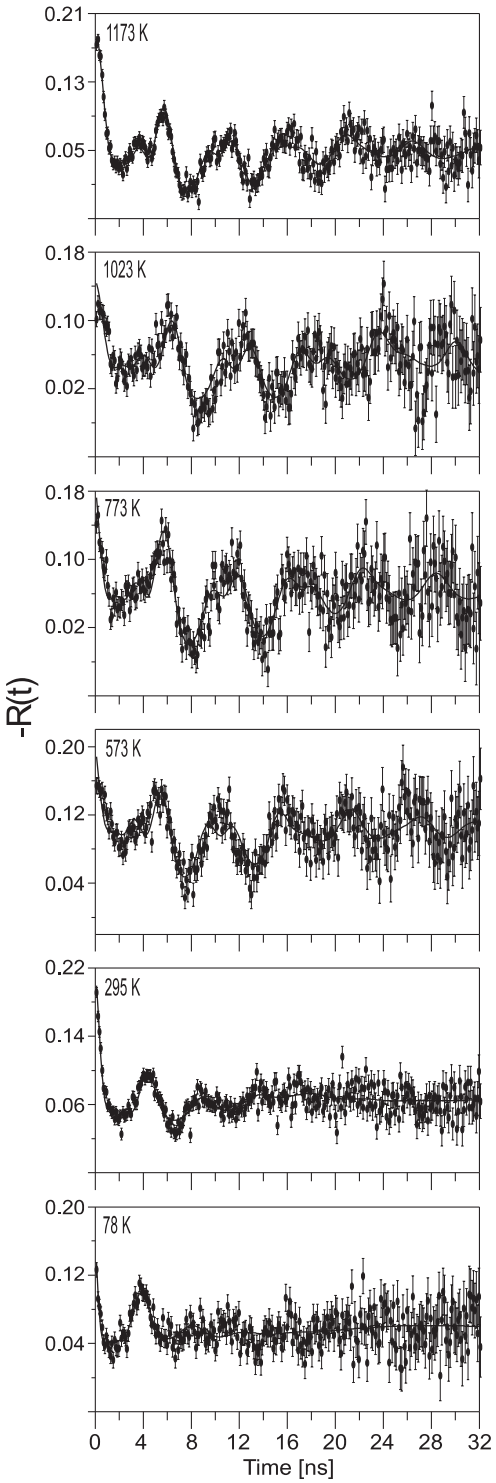

Figure 2. TDPAC spectra of ^{181}Ta in the intermetallic compound Hf_2Co at six selected temperatures.

Table 2. The parameters of the Hf_2Co structure. The distances are in Å.

	Number of bonds	Experiment[a]	WIEN97
u		0.2142(3)	0.221
v		0.816(1)	0.813
16c			
Hf1–Co	6	2.656(9)	2.714
Hf1–Hf2	6	3.081(3)	3.103
48f			
Hf2–Co	2	2.77(2)	2.657
Hf2–Co	2	3.060(4)	3.076
Hf2–Hf1	2	3.081(3)	3.103
Hf2–Hf2	4	3.198(2)	3.195
Hf2–Hf2	4	3.256(2)	3.211

[a] Reference [6].

4. Calculations of the EFGs

4.1. Method of computation

In order to get more detailed information about the origin of the EFG in this compound, *ab initio* calculations employing the LAPW method within the framework of the density functional theory were performed by means of the WIEN97 program [5]. In the LAPW method the unit cell is partitioned into muffin-tin (MT) spheres centered at the atomic positions, and an interstitial region. The Bloch wavefunctions are expanded using plane waves that are augmented by atomic-like functions inside the spheres. The calculations were performed for the experimental lattice parameter ($a = 12.066$ Å).

The generalized gradient approximation in the parameterization of Perdew–Burke–Ernzerhof [10] was employed. The LAPW sphere radii R_{mt} were 1.333 and 1.317 Å, for Hf and Co, respectively. The Hf 6s, 6p, 5d, 4f and Co 4s, 4p, 3d states were put in the valence panel. The standard LAPW basis set is extended with local orbitals [17]. They were employed for the Hf 5s, 5p and Co 3p semicore states. The Brillouin zone (BZ) integration was performed using a k mesh of 512 points, which is reduced to 29 special k points in the irreducible BZ wedge. The plane wave cutoff parameter $R_{mt}K_{max}$, which is often used as a measure of the quality of the LAPW calculation, was set to 7.7.

4.2. Structural relaxation and electronic structure of Hf_2Co

Before calculating the electronic structure, we relaxed the internal parameters of the structure, keeping the experimental lattice constant fixed. Starting from the experimental values for the structural parameters, we calculated the Hellmann–Feynman forces acting on Hf2 and Co atoms. The Hf1 atoms are fixed, owing to symmetry restrictions. According to the calculated forces, the atoms were allowed to move along the symmetry directions. The relaxation was carried out until the forces were smaller than 0.04 eV $Å^{-1}$. The calculated values of the parameters u and v, as well as the distances around Hf1 and Hf2, are reported in table 2.

The total density of states (DOS) for the relaxed Hf_2Co structure, along with the site projected and l-decomposed DOS, is shown in figure 3. The gross features of the Hf_2Co DOS are quite similar to the DOS of the isostructural compound Hf_2Fe [11]. Hf 4f bands situated about 12 eV below the Fermi level (E_F) are not presented in figure 3. The energy dispersion of these bands is small, indicating their low hybridization with the other valence electrons.

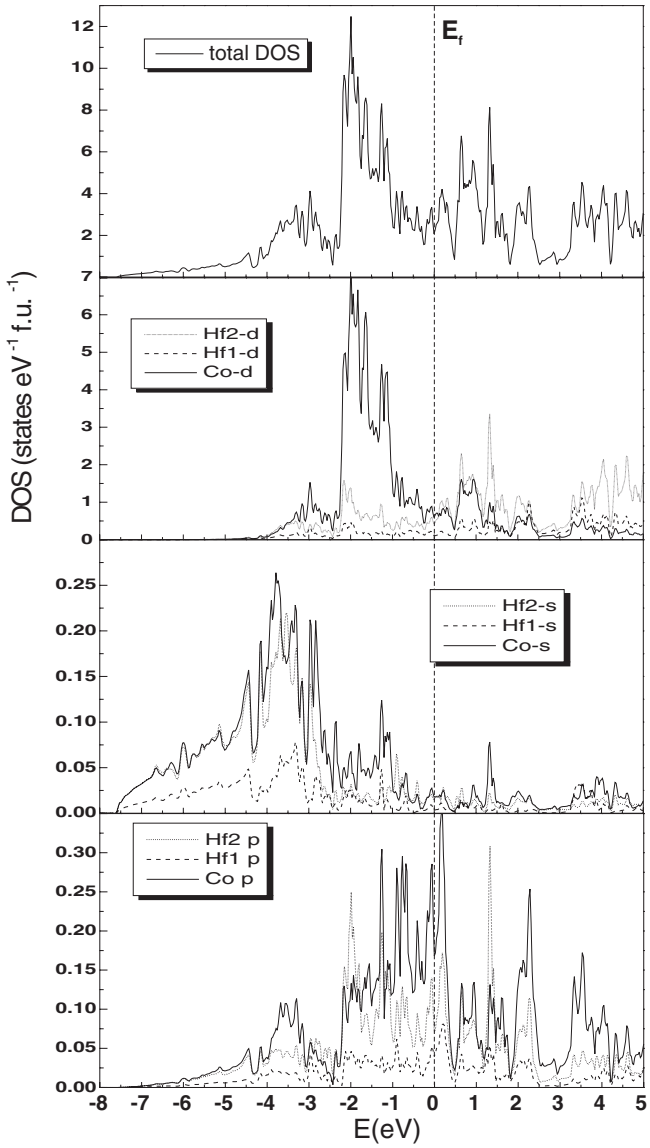

Figure 3. Total (top) and site projected (bottom) density of states for the relaxed structure of Hf_2Co intermetallic compound.

They also retain almost all of their electrons (see table 3). The DOS in the energy region from -8 to -4 eV is predominantly of s character. From about -4 eV up to the E_F the DOS is of pronounced d character. There is a strong mixing of Co 3d and Hf 4d orbitals throughout this region. The same is true for the p electrons of all constituent atoms. This overlap over large energy ranges seems to be a common feature of the atom-projected DOS of this compound and Hf_2Fe [11]. Figure 3 reveals that Co 3d electrons give the major contribution to the DOS of the central valence region. As we approach the E_F, the contribution from the Hf2 d and p electrons becomes more prominent and of the same order as that of the Co d and p electrons. Since the number of Hf1 atoms in the unit cell equals one third of the number of Hf2 atoms, their contribution to the DOS is correspondingly smaller.

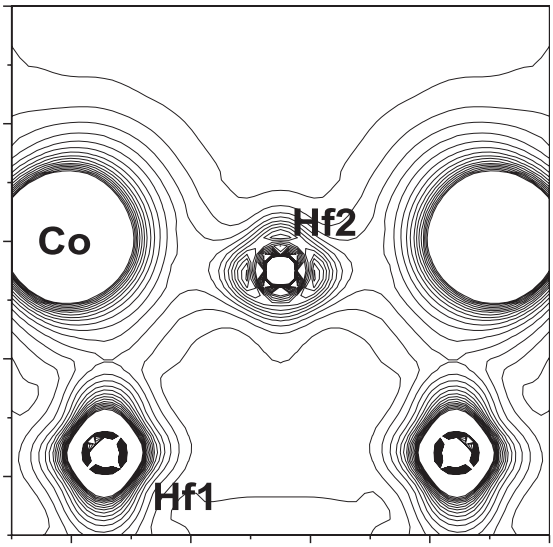

Figure 4. The charge density for Hf_2Co in the plane passing through Hf1, Hf2 and Co (atoms labelled in figure 1-bottom) with 20 contours drawn between 0 and 0.1 electrons au^{-3}.

Table 3. The *l*-decomposed site projected charge (in electrons) inside the muffin-tin spheres around Hf1, Hf2 and Co in Hf_2Co.

Atom	s	p	d	f
Hf1	2.316	6.071	1.397	13.984
Hf2	2.303	6.084	1.314	13.977
Co	0.595	6.519	7.492	0.019

Additional information can be gathered by analysing the charge confined in the MT spheres, around the non-equivalent atomic sites. The construction of the MT spheres is not unique, and the charge contained within by no means corresponds to the actual ionic charge. Also, the charge in the interstitial region cannot be assigned to any particular atomic species. Still, this information can be useful to get an overall picture about possible charge transfer between constituent atoms. Table 3 reveals the site projected partial charge inside the MT spheres around Hf1, Hf2 and Co. One can see that the s charge of Hf1, Hf2 and Co, as well as the d charge of Hf1 and Hf2, is redistributed, filling mostly the Co d and p states, and the interstitial region. This charge transfer is an indication that the bonds in this metallic compound could also have partly ionic character.

Figure 4, where we present the valence charge density around the Hf2 atom, provides further insight into the bonding properties of this compound. One can see large aspherical charge distortions in the region between the Hf1(Hf2) and Co atoms. This is an indication of covalent bonding. Therefore, we can conclude that the bonds in Hf_2Co are not purely metallic, but rather a mixture of metallic, covalent, and ionic contribution.

4.3. The electric field gradient in Hf_2Co

After the decay of ^{181}Hf, the EFG is actually measured on the daughter nucleus ^{181}Ta. Since only several ppm of Hf atoms are activated, the Ta concentration in the samples is rather small. In such a situation, the supercell method is usually used to simulate the experimental condi-

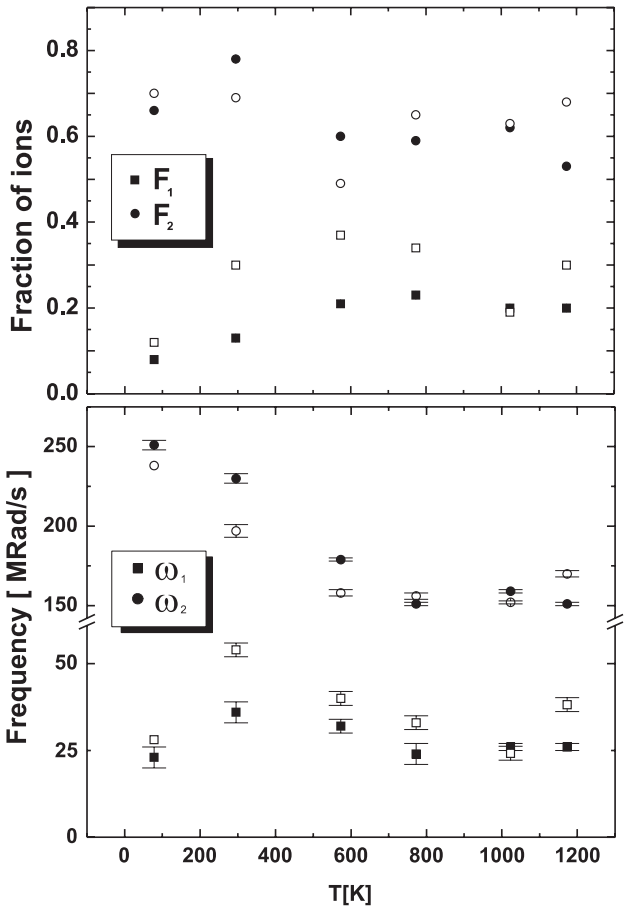

Figure 5. Fraction of ions occupying the 16c (F_1) and 48f (F_2) position as a function of temperature (top), along with the temperature dependence of the interaction frequencies ω_{Q_i} (bottom). The values of the corresponding parameters obtained by fixing the η_1 parameter to zero are given with open symbols.

tions. To perform a calculation with the accurate LAPW method on a supercell of 96 atoms (which is a minimum for a reliable calculation in this case) would be computationally quite formidable task. Hence, we follow the approach of [11], computing the EFGs on the Hf atoms in the original primitive unit cell. The justification for this approach comes from the fact that the major EFG contribution in many systems with Hf comes from its p electrons. Since Ta has only one d electron more than Hf, their radial p functions should be similar [21]. However, this approach does not take into account the possibility of lattice relaxation that may take place after the replacement of Hf with Ta. It is a well established fact, confirmed by many theoretical and experimental studies [23] of different systems, that the EFG parameters are particularly sensitive to changes in the interatomic distances of the nearest atomic shells around the probe atom.

After the relaxation of the Hf_2Co structure we analysed the EFG at both crystallographic positions, decomposing it into several different l–l' contributions [18], as summarized in table 4. The lattice contribution to the EFG is negligibly small at both positions. The deviation of the valence charge density in the vicinity of the Hf nucleus from spherical symmetry makes the main contribution to the EFG. Owing to the additional local orbitals that are employed for accurate treating of the low-lying semicore electrons, we also calculated their contribution

Table 4. Decomposition of the calculated V_{ZZ}-values, in units of 10^{17} V cm^{-2}.

	s–d	6p–6p	5p–5p	d–d	Others	Total
16c						
	+0.12	+1.77	−4.44	+2.29	−0.18	−0.44
48f						
	−0.33	−21.69	6.48	−2.88	0	−18.42

Table 5. Some measured and calculated EFG parameters in Hf_2Co. V_{ZZ} is given in units of 10^{17} V cm^{-2}.

	Measured (78 K)	Calculated (0 K)	
	^{181}Ta	Hf	Ta
V_{ZZ}			
16c	±2.4	−0.4	−1.6
48f	±26.1	−18.4	−26.7
η			
16c	0.74	0	0
48f	0.04	0.43	0.28

to the EFG. Apart from the expected 6p–6p contribution, we found that there is sizable contribution from the semicore 5p electrons, as predicted in [22]. At the 16c position the low magnitude of the calculated EFG originates from the cancellation of this semicore and valence d and 6p contributions. At the 48f position the dominant contribution comes from the 6p valence electrons, and the semicore 5p contribution is again of opposite sign to the valence p and d contributions. The value of the EFG at this position is an order of magnitude higher than the EFG at the 16c position in accordance with the experimental observation. The strong asymmetry of the charge density in the region close to the Hf2 nuclei (figure 4) is the origin of the large value of the EFG at this position. In order to estimate the Ta impurity effect, we calculated the EFGs in two hypothetical compounds: $Hf1_{0.375}Ta_{0.125}Hf2_{1.5}Co$ and $Hf1_{0.5}Hf2_{1.375}Ta_{0.125}Co$, where Ta replaces, respectively, the Hf1 and Hf2 atom in the Hf_2Co primitive unit cell. The resulting conventional unit cells thus contain four Ta atoms. Both the point-group symmetry around the Ta atom and the shell structure up to a distance of 8.531 Å are the same as those around Hf1(Hf2) position in Hf_2Co. However, the number of non-equivalent positions within the unit cell is larger and the complexity of the calculations increases. We allowed for the atoms presented in figure 1 to relax until the forces were smaller than 0.12 eV Å^{-1}. As a result of a strong interaction between Ta and the NN Co atoms at both positions, the NN distances are strongly reduced. The NN Ta_{Hf1}–Co distance was found to be ∼3% shorter than the Hf1–Co distance in Hf_2Co. The relaxation of the NN Ta_{Hf2}–Co distances is even more pronounced, resulting in ∼3.8% shorter bonds. The calculated EFGs and ηs at both positions are given in table 5. Although for definite conclusions supercell calculations have to be performed, we can say that, compared to the measured values, the calculated V_{ZZ} at both positions, and η at Ta_{Hf2}, are improved over the corresponding calculated values in Hf_2Co.

5. Summary and conclusions

The results of the TDPAC measurements are systematically fitted with two different interactions that correspond to the two different crystallographic positions (16c and 48f) of the probe ion in the unit cell of Ti_2Ni type, and a sizable fraction of ions, $F_0 = 1 - (F_1 + F_2)$ (table 1), which

do not contribute to the interactions. The use of another high frequency interaction observed also in the isostructural Hf_2Fe [19, 20] was absolutely necessary only at low temperatures for the samples that were not adequately thermally treated. We believe that the reason for its appearance is the high concentration of defects and/or incomplete formation of the Ti_2Ni phase in those samples. In these cases, the frequency ratio between the two high frequency interactions ($\sim$1.3) is similar to that observed in Hf_2Fe [20], and their relative abundance strongly depends on the thermal history of the sample. The previous investigations [1, 6–8, 12, 13] of this type of compounds show that complete formation of the Ti_2Ni phase is not easy to achieve, except probably for the Hf_2Fe system.

As seen from the TDPAC spectra (figure 2), the main contribution to the precession pattern is due to the high frequency component ω_{Q2}, which is related to the 48f lattice site. The low frequency component ω_{Q1} is assigned to the 16c lattice site. The temperature dependence of ω_{Q1} (figure 5), with a pronounced maximum at low temperatures, is rather unusual for a metallic system. Owing to the small number of experimental points, the position of the maximum cannot be determined precisely from the presented measurements. The temperature range is essentially the same as that established with $C_p(T)$ measurements in the isostructural phases Hf_2Co, Hf_2Fe and Hf_2Rh [13], as well as with TDPAC in Hf_2Fe and Hf_2Rh [16]. However, due to the relatively high δ and low population F_1 of this lattice site, this short discussion regarding the ω_{Q1} temperature dependence should be taken with caution.

The large value of the parameter δ, especially at the 16c site and at low temperatures, and a large fraction of probe ions that do not contribute to the interactions, support the assumption that the structure of this compound is not well ordered at and below room temperature. Above it, the ratio F_2/F_1 is close to 3, as expected for this structure type, but F_0 is relatively large, which indicates that besides the Ti_2Ni, a sizable amount of a disordered phase still exists. Both the EFG and δ temperature behaviour indicate local relaxation of the structure with increasing temperature.

We also checked the possibility of fitting the data by fixing the η at the 16c position to the theoretically expected value $\eta = 0$. The values of the EFG parameters at both positions, obtained that way, are presented in figure 5 by open symbols. Besides the fact that the quality of the fits is worse (e.g., $\chi^2_{78\ \mathrm{K}}$ =291, for η_1-free, and $\chi^2_{78\ \mathrm{K}} = 363$, for η_1 fixed to zero), the values of δ and F at certain temperatures are unphysically high (i.e., $\delta_{16c} > 0.35$, $F_{16c} > 0.25$). We decided to accept the η_1-free results. It should be noted that for η_1 fixed to zero the temperature dependence of the EFG at both positions is preserved.

Our calculations show that the low point-group symmetry around the Hf2 site, combined with a relaxation of the neighbouring atoms, leads to a strong anisotropy of the valence charge density and consequently to a high value of the EFG (figure 4). For the 16c position the calculated values substantially differ from the corresponding experimental ones. However, the low magnitude of the EFG is clearly reproduced. If we consider the calculated values at Ta in the hypothetical Hf–Ta–Co compounds, the agreement with the experimental values is even better. Moreover, our calculations show that, like in some other complex intermetallic systems [24], the impurity effect is strongly correlated to the local lattice relaxation around the impurity atom. In addition, the fact that the value of the measured η_1 differs from zero suggests that the local symmetry around Ta at the 16c position is changed. Due to their complexity any possible symmetry breaking calculations have not been considered in this study.

The decomposition of the EFG tensor, using the FP-LMTO(ASA) method [11, 15], has shown that the 5d electrons of Hf give a predominant contribution at the 16c site, and the 6p Hf electrons at the 48f site. These studies have also emphasized the fact that there is a substantial hybridization between the 5d Hf and 3d Cd(Fe) electrons. Our calculations confirm the latter of these observations, and to some extent the former (relatively large d–d contribution to V_{ZZ}),

but we found that the dominant contribution at the 16c site also comes from the p electrons. We also demonstrated that in the calculation of the EFGs the lattice relaxation should be included, which has not been the case in previous LMTO studies. We came to the conclusion that the contribution from the semicore states to the EFG is far from negligible, and must be taken into account. The quantitative agreement between the theoretical results and the experimental data is acceptable, but for really precise comparisons the supercell calculations are necessary.

The treatment of the electronic 4f states also deserves some attention. We performed additional calculations treating the 4f states as atomic-like core states (open-core treatment) switching off the hybridization between 4f and valence states. In contrast to the earlier FP-LMTO-ASA calculation of the isostructural compound Hf_2Fe [11], we found that the physical quantities of interest are not substantially changed for the two different treatments of the 4f states. Comparing the differences obtained by the two methods, we must emphasize here that the FP-LAPW method is numerically more precise and less sensitive to the details of calculation, such as, for instance, the choice of the MT sphere radii.

Acknowledgment

This work was supported by the Serbian Ministry of Science, Technologies, and Development under Grant No. 2021.

References

[1] Baudry A, Boyer P, Chikdene A, Harris S W and Cox F S 1990 *Hyperfine Interact.* **64** 657
[2] Baudry A, Boyer P, Ferreira L P, Harris S W and Pontonnier L 1992 *J. Phys.: Condens. Matter* **4** 5025
[3] Mukai D, Miyata H and Aoki K 1999 *J. Alloys Compounds* **293–295** 417
[4] Bedi S C and Forker M 1993 *Phys. Rev.* B **47** 14948
[5] Blaha P, Schwarz K and Luitz J 1999 *WIEN97, a Full Potential Linearized Augmented Plane Wave Package for Calculating Crystal Properties* Vienna University of Technology, Vienna 1977
This is an improved and updated UNIX version of the original copyrighted WIEN code, which was published by Blaha P, Schwarz K, Sorantin P and Trickey S B 1990 *Comput. Phys. Commun.* **59** 399
[6] Cekić B, Mitrić D, Ivanović N, Mitrić M, Koički S and Manasijević M 1993 *Matica Srpska, Proc. Natural Sci.* **85** 243
[7] Cekić B, Koički S, Rodić D, Manasijević M and Prelesnik B 1988 *Hyperfine Interact.* **39** 303
[8] Buschow K J, Wernick J H and Chin G Y 1978 *J. Less-Common Met.* **59** 61
[9] Frauenfelder H and Steffen R M 1965 *Alpha-, Beta-, and Gamma-Ray Spectroscopy* (Amsterdam: North-Holland)
[10] Perdew J P, Burke S and Ernzerhof M 1996 *Phys. Rev. Lett.* **77** 3865
[11] Lalić M V, Popović S Z and Vukajlović F R 1999 *J. Phys.: Condens. Matter* **11** 2513
[12] Cekić B, Ivanović N, Rakočević Z, Koteski V, Manasijević M and Koički S 1998 *J. Appl. Phys.* **84** 4842
[13] Ivanović N, Rodić D, Cekić B, Manasijević M, Koički S, Babić D and Nikolić R 1995 *J. Mater. Sci.* **30** 3547
[14] Koički S, Cekić B, Ivanović N, Manasijević M and Babić D 1993 *Phys. Rev.* B **48** 9291
[15] Lalić M V, Popović Z S and Cekić B 1998 *SFIN* vol 11 (A2) ed R Antanasijević and I Aničin (Belgrade: Institute of Physics) p 147
[16] Ivanović N, Koički S, Cekić B, Manasijević M, Koteski V and Marjanović D 1999 *J. Phys.: Condens. Matter* **11** 289
[17] Singh D 1991 *Phys. Rev.* B **43** 6388
[18] Blaha P, Schwarz K and Dederichs P H 1990 *Phys. Rev.* B **37** 2792
[19] Akselrod Z Z, Komissarova B A, Kryukova L N, Ryasnyi G K, Shpinkova L G and Sorokin A A 1990 *Phys. Status Solidi* b **160** 255
[20] Van Eek S M and Pasquevich A F 1999 *Hyperfine Interact.* **122** 317
[21] Terrazos L A, Petrilli H M, Marszalek M, Saitovitch H, Silva P R J, Blaha P and Schwarz K 2002 *Solid State Commun.* **121** 525
[22] Ehmann J and Fähnle M 1996 *Phys. Rev.* B **55** 7478
[23] Kaufmann E N and Vianden R J 1979 *Rev. Mod. Phys.* **51** 161
[24] Motta A T, Cumblidge S E, Catchen G L, Legoas S B, Peasano A and Amaral L Jr 2001 *Phys. Rev.* B **65** 014115